

Tests to Prove Performance of High Temperature Water Jet Compressor

By Paul L. Geiringer and Lloyd T. Taylor, American Hydrotherm Corporation, New York, New York, for Office of Saline Water; J. A. Hunter, Director, and Everett N. Sieder, Chief, Distillation Division.

Contract 14-01-0001-948

UNITED STATES DEPARTMENT OF THE INTERIOR • Stewart L. Udall, Secretary
Max N. Edwards, Assistant Secretary for Water Pollution Control

For sale by the Superintendent of Documents, U.S. Government Printing Office
Washington, D.C. 20402 - Price 45 cents

Created in 1849, the Department of the Interior—America's Department of Natural Resources—is concerned with the management, conservation, and development of the Nation's water, wildlife, mineral, forest, and park recreational resources. It also has major responsibilities for Indian and Territorial affairs.

As the Nation's principal conservation agency, the Department of the Interior works to assure that nonrenewable resources are developed and used wisely, that park and recreational resources are conserved for the future, and that renewable resources make their full contribution to the progress, prosperity, and security of the United States—now and in the future.

FOREWORD

This is one of a continuing series of reports designed to present accounts of progress in saline water conversion and the economics of its application. Such data are expected to contribute to the long-range development of economical processes applicable to low-cost demineralization of sea and other saline water.

Except for minor editing, the data herein are as contained in a report submitted by the contractor. The data and conclusions given in the report are essentially those of the contractor and are not necessarily endorsed by the Department of the Interior.

F I N A L R E P O R T

TESTS TO PROVE PERFORMANCE

OF HIGH TEMPERATURE WATER JET COMPRESSOR

PREPARED FOR

UNITED STATES DEPARTMENT OF THE INTERIOR

OFFICE OF SALINE WATER

Contract No. 14-01-0001-948

by

AMERICAN HYDROTHERM CORPORATION

470 Park Avenue South
New York, N.Y. 10016

December 15, 1967

TABLE OF CONTENTS

	<u>PAGE</u>
I. INTRODUCTION	1
II. SUMMARY OF TEST RESULTS	2
III. DESCRIPTION OF TEST EQUIPMENT AND PROCEDURE	2
IV. TEST RESULTS AND DATA	7
V. ANALYSIS OF DATA	10
VI. SUMMARY	16

LIST OF FIGURES

1. SCHEMATIC OF TEST ARRANGEMENT
2. SCHEMATIC OF INSTRUMENTATION
3. PHOTOGRAPHS - TEST JET
4. PHOTOGRAPHS - TEST JET
5. PHOTOGRAPHS - TEST JET
6. PHOTOGRAPHS - TEST JET
7. MATERIAL & ENERGY BALANCE FOR HTW JET
8. NEEDLE VALVE CALIBRATION
9. TEST JET DIMENSIONS
10. HTW NOZZLE DESIGN
11. TEST DATA SUMMARY
12. TEST DATA - 61.8 mm NOZZLE
13. TEST DATA - 61.8 mm NOZZLE
14. TEST DATA - 61.8 mm NOZZLE
15. TEST DATA - 61.8 mm NOZZLE

LIST OF FIGURES - Continued

16. ANALYSIS TEST DATA - 61.8 mm NOZZLE
17. PRESSURE PROFILE TEST NO. 104
18. TEST DATA ANALYSIS - 76.2 mm NOZZLE
19. TEST DATA ANALYSIS - 76.2 mm NOZZLE
20. COMPRESSION PROCESS ON h-s DIAGRAM

ABSTRACT

American Hydrotherm Corporation offered to warrant, design and build a high temperature water jet compressor to produce not more than 1.3 lbs of compressed steam for each pound of suction steam using saturated water at 1010 psia as a driving medium when compressing steam from 20.5 to 25 psia. On request of OSW, tests were conducted to confirm that this performance could be achieved.

Test results reported here show the actual performance was considerably better than the above. The tests proved that using 1010 psia saturated high temperature water, one lb of saturated steam can be compressed from 20.77 psia to 25.46 psia, while using 0.757 lbs of high temperature water and producing only 1.26 lbs of 25.46 psia steam at the discharge, or 0.26 lbs of "excess" steam. The capacity of the test jet was 50,000 lbs/hr of suction steam.

It is expected that a further reduction in the amount of driving fluid, HTW, 10 to 20%, can be expected thru a continuation of the test work.

I. INTRODUCTION

The vapor compression distillation process for desalination has a relatively low energy requirement. However, in the conventional vapor compression process, energy is required as expensive "high grade" shaft work. Also, the process involves complex mechanical equipment which increases investment and operating costs.

Based on available data and designs, American Hydrotherm Corporation suggested that a HTW jet compressor be used for desalination to reduce these costs. It was proposed that a HTW jet compressor be installed at the Freeport, Texas plant or at one of the other OSW demonstration plants. Performance data for such a compressor were submitted to the Office of Saline Water. Since the jet had to be installed on these large plants and considerable other investments had to be considered, OSW desired that the performance offered by American Hydrotherm should be proven by actual test on a large model. This was the purpose of the test work reported here.

The test model was designed for compressing vapor from 20.5 to 25.0 psia. For this pressure range the performance anticipated was 1.30 lbs of discharge steam for each pound of suction steam. However, since the results of the test jet could be scattered, and since the time allowed for completion of the test was very short, a 15% higher performance of discharge steam was guaranteed.

The test ejector was designed and built in the U.S.A. and tests were conducted in France on an existing test stand available to American Hydrotherm Corporation.¹ The nominal capacity of the test stand was 50,000 lbs per hour of suction steam.

1. Tests were conducted at the S.N.E.C.M.A. (Societe Nationale D'Etude et de Construction de Moteurs D'Aviation) research and development center, Villaroche, France.

II. SUMMARY OF TEST RESULTS

Test data show that the performance of the HTW jet compressor was considerably better than the contract requirements. Test performance is compared with the minimum required performance in the following tabulation.

	<u>PREDICTED PERFORMANCE</u>	<u>TEST RESULTS</u>
Suction Pressure psia	20.5	20.77
Discharge Pressure psia	25.0	25.46
<u>Wt. excess discharge steam</u> Wt.suction steam	0.30 - .50	0.265

Two high temperature water nozzles with discharge diameters of 61.8 and 76.6 mm, respectively, were tested. The best performance was attained with the smaller discharge nozzle.

More complete performance data for the point of best performance is given in Section IV.

III. DESCRIPTION OF TEST EQUIPMENT AND PROCEDURE

A. TEST APPARATUS ARRANGEMENT

The arrangement of the test equipment is shown in Figure 1. Water is electrically heated and stored in the HTW accumulator. At the start of the test, a hydraulic needle valve at the HTW nozzle is opened to a predetermined position. In passing through the driving nozzle the high temperature water (543°F, 1010 psia) flashes with a corresponding decrease in enthalpy and an increase in velocity. The suction vapor entering the mixing section is also accelerated by expansion through the converging annular area. The high velocity water-vapor mixture leaving the nozzle mixes with the suction vapor. In the mixing chamber the vapor velocity is further increased by momentum exchange with the high

velocity water in the converging section of the jet. In the diffuser section (diverging section), the velocity is decreased and the decrease in kinetic energy causes an increase in the pressure and enthalpy of the vapor.

Since a portion of the high temperature water flashes to vapor, the quantity of compressed steam leaving the diffuser is greater than the quantity of suction vapor entering. The additional vapor is called "excess" steam.

The mixture of compressed vapor and water is separated by a change of direction in the twin separators. The excess steam is then vented from the system through pressure control valves. The remaining vapor is recycled through a pressure reducing station to the compressor inlet. The recycled vapor contains some entrained water which tends to desuperheat the suction steam at the pressure reducing valve. For application in a desalting process the excess steam would be used as the heating medium for a conventional multiple effect or multi stage-flash evaporator.

Photographs of the test stand are shown in Figures 3,4,5, and 6. Figures 3 and 4 show the diffuser section, separators and other equipment located outside the test stand building. The remaining parts of the test stand are located inside the building.

B. DESCRIPTION INSTRUMENTS AND CONTROLS

1. Suction and Discharge Pressure Control

The suction pressure of the ejector can be adjusted by means of a pneumatically operated remote control butterfly valve. To reduce the pressure variation produced by this valve, the damper has been perforated by 18 drillings of 1-inch diameter and twenty drillings of 5/8-inch diameter. To improve and streamline the inlet flow, two simple turning vanes are installed in the 90° ell at the compressor suction. Unfortunately, the important inner turning vane was not installed so that the flow into the ejector was more turbulent than desired.

The discharge pressure is controlled by regulating the excess steam discharge to the atmosphere. This is done by an automatic pressure controller which operates a 5" ball valve. Also, a 5" hand valve is provided to assure that the automatic valve can operate in the desired flow range.

2. Flow and Pressure Measurements

All pressure measurements are shown schematically in Figures 1 and 2. Pressures were registered by mercury manometers. The manometers were arranged to provide an equal head of water on each side of the manometer at zero differential pressure. In some cases, calibrated pressure gages were used to check the manometer readings. All pressure indicators, along with a clock, were mounted on a single panel. Data could be recorded manually or by a camera mounted in front of the board.

Two flow rates are actually determined during the test. These are the suction vapor flow, G_2 , and the HTW flow from the accumulator, G_1 . Other flows, the excess exhaust steam, G_3 , and the water return flow from the separator, are determined by calculating an energy and material balance based on the two measured flow rates and the conditions leaving and entering the jet. For the design suction and discharge pressure the material and energy balance relations are shown graphically in Figure 7.

The suction vapor flow was measured by an orifice meter. The pressure drop across the orifice was measured by a Meriam Flow Meter and also by U-tube manometers, as shown in Figure 2.

The HTW flow was measured by determining the level change in the accumulator in a measured time period and by calibrating the needle valve. The amount of water in the accumulator before and after the tests was determined by means of a differential pressure gage M_6 of Figure 2. The test duration time was measured simultaneously. The opening of the needle valve to a predetermined position is obtained by means of a

hydraulically operated, quick opening device. The HTW flow rate, is computed as follows:

$$G_1 = \frac{\text{outflowing water quantity}}{\text{test time}}$$

The value reported for G_1 is a mean value since the accumulator content, as well as the accumulator pressure, is reduced without introducing any energy. Therefore, G_1 , is related to the mean HTW pressure. Typical test data are shown in the following tabulation.

TYPICAL TEST DATA FOR HTW FLOW AND PRESSURE

Pressure in HTW Accumulator

	At Start	At End	Mean Value	Draw-off from HTW Quantity
kg/cm ²	92	80	86	512 kg
psia	1310	1138	1223	1,130 lbs
kg/cm ²	77	65	71	408 kg
psia	1095	924	1010	900 lbs

Figure 8 shows data for the needle valve calibration. Tests were made using each of the two HTW nozzles with HTW pressures of 1010 psia and 1223 psia. The data show that the difference in shape of the two nozzles has no effect on the flow through the nozzle. Figure 8 also shows the static pressure at a point 3.5 mm from the discharge end of the nozzle.

It is interesting to note that the nozzle efficiency can be calculated from the data of Figure 8, assuming that one direction flow and uniform velocity of the

liquid and vapor exist. However, calculations based on these assumptions show over 100% efficiency which indicates that the assumptions are not valid. The velocity profile across the nozzle is unknown and it is doubtful that the water drops are moving with the same velocity as the steam.

C. TEST JET DIMENSIONS

The important dimensions of the test ejector are shown on the outline sketch in Figure 9.

The shape of the HTW driving nozzle is shown in Figure 10. The nozzle can be combined with two end pieces with discharge diameters of 61.8 and 76.2 mm respectively.

Near the end of each driving nozzle, a pressure tap was installed to determine the static discharge pressure at various flow rates.

D. METHOD OF OPERATION

Prior to each test, the whole ejector system is purged and preheated with steam. In this way, since the equipment is well insulated, the temperature of the metal is raised to approximately the operating temperature. This eliminates high thermal stress in the equipment and reduces condensation of vapor during the test.

Since continuous operating time is short, the HTW flow, suction and discharge pressure are held constant in each run. During the first part of the test, there is a short time to make final adjustments to obtain desired conditions. Observations and photographs of the indicating instruments and clock show when steady state conditions are achieved.

IV. TEST RESULTS

A. GENERAL

Numerous tests, over 160, were conducted to determine

(1) the characteristics of the particular configuration at the design point (20.5 psia suction pressure), and

(2) the combination of flow rates for each configuration at which the best performance occurred.

Tests were conducted using both driving nozzle diameters, 61.8 mm and 76.2 mm respectively. Early test showed that the smaller driving nozzle produced the best results in the desired pressure range.

In applying the HTW jet in a vapor compression desalination process, it is desirable to obtain the highest rise in saturated temperature in the suction vapor while using the least amount of driving water or producing the least amount of excess steam. That is, the ratio shown below would have a minimum value:

$$(1) \text{ performance ratio} = \frac{G_3/G_2}{t_2-t_1}$$

Where:

G_3 is the excess steam weight at the discharge pressure

G_2 is the suction steam weight

t_2-t_1 is the difference in suction and discharge temperature of the vapor

The above ratio is used here as a convenient factor for evaluating and comparing performance of the test jet under various conditions. For the narrow range of pressures discussed here the performance ratio is approximately inversely proportional to the over-all efficiency.

The test data for the flow and pressure conditions where maximum performance occurred are tabulated in Figure 11. The point of best performance for the smaller driving nozzle, 61.8 mm diameter, was at a higher suction pressure than the best performance point for the larger driving nozzle.

B. TEST DATA FOR THE 61.8 mm DRIVING NOZZLE

Tests were conducted in groups in the following way. In each group of tests, the HTW flow rate was set at one desired value for all tests in the group. This was done by opening the calibrated valve at the driving nozzle to a measured value, "dimension a". Then for each increment of HTW flow rate, a group of tests was conducted at various suction flow rates and suction pressures. The discharge pressure in each group of tests was held approximately constant.

The data for the tests on the 61.8 mm nozzle are shown graphically in Figures 12, 13, 14 and 15. For HTW flow rates 8.42, 9.5, 10.44 and 10.8 lbs/sec respectively. As a convenience for spreading the data, the various values are plotted against the opening of the valve in the vapor recycle line. Both measured and calculated flows are shown for each test run.

In Figure 16, the performance ratio, excess steam divided by temperature rise, is plotted for all the groups of tests on the 61.8 mm nozzle. These curves show that the lowest value of the "performance ratio", highest efficiency, occurs in the test group made at the highest HTW flow rate, 10.8 lbs/second. Data from this test group are shown in Figure 15. In test runs 120 through 123, the ratio of G_3/G_2 to (t_2-t_1) is about 0.0238. Similar values occurred in the tests at a HTW flow of 10.44 lbs/second shown in Figure 14.

Tests at higher HTW flow rates were not possible because the volume of the HTW accumulator did not allow a test duration required for reaching steady state flows through the jet. Tests at higher and lower discharge pressures would also be desirable to completely determine the most efficient operating conditions.

Wall pressure along the axis of the jet was measured in several tests. A typical example of the resulting pressure profile is shown in Figure 17. The data are from Test 104. Using the pressure profile and assuming flow in one direction parallel to the jet axis and that the liquid and vapor velocity are equal, the efficiency of the diffusor could be calculated. However, based on the data and these assumptions, the diffusor is almost 100% efficient, which is unrealistic. This and other factors do, however, suggest that the greatest losses are in the mixing section.

C. TEST DATA FOR THE 76.2 mm DRIVING NOZZLE

Tests on the larger driving nozzle were conducted in groups with constant HTW flow as was done with the smaller nozzle. Also, two discharge pressures were explored.

Tests on the 76.2 mm nozzle produced a poor performance ratio when operating at approximately the design discharge pressure. However, in the lower pressure range, the performance approached that of the smaller nozzle.

The data on the large nozzle are summarized for the "high" and "low" pressure test in Figures 18 and 19 respectively.

In the tests with lower discharge pressure, the best performance ratio was 0.0241. This was reached at an intermediate HTW flow rate of 7.7 lbs/sec. However, in tests at the higher design discharge pressure the performance was poor and the performance ratio was up to 0.0272. This occurred at the highest HTW flow rate possible. The curves in Figure 18 show that a better performance ratio may probably be reached if higher HTW flow rates were tested. This was not practical in the existing test stand because of the limited hot water accumulator volume.

V. ANALYSIS OF DATA

The test results show the performance of a HTW jet of a given geometric configuration when operating at various conditions of HTW flow, suction pressure and discharge pressure. The data also show the flow conditions at which the best performance occurs for this particular jet. It is desirable to reduce these data to a general measure of efficiency which would be useful in predicting performance of HTW jets designed for new conditions, in evaluating competitive jets, and in applying the jet to various processes. Also, for development purposes, it is also desirable to know the efficiency or effectiveness of each component of the test jet in order to establish priorities for design improvements.

Several definitions of efficiency are applicable and useful. These are discussed and defined in the following paragraphs.

The jet compression process is shown in Figure 20 on an exaggerated enthalpy-entropy diagram. The isentropic processes are shown by means of solid lines and real processes by dotted lines. The line "AC", connecting the initial states of the two inlet streams, represents the theoretical reversible mixing line. If a reversible process takes place, the mixture would be defined by a point somewhere on this line. The exact location would depend on relative quantities and conditions of the two entering streams. The horizontal line at h_m^o is the stagnation enthalpy resulting from the mixing of two streams. The final enthalpy of the mixture at rest, no matter what the mixing process, will be at this value. The value h_m^o depends only on the respective quantities and initial stagnation enthalpy of the driving and driven streams, h_1^o and h_2^o respectively, as expressed by the equation below.

$$(2) \quad h_m^o = \frac{G_1 h_1^o + G_2 h_2^o}{G_1 + G_2}$$

For a reversible process the entropy of the mixture leaving the jet would be defined by the point where line "A-C" intersects the constant enthalpy line, h°_m . This point would also define the final discharge pressure, P_5 , for a reversible process. The entropy of the final discharge mixture for the reversible process may also be computed from the equation below.

$$(3) \quad s_5 = \frac{G_1 s_1 + G_2 s_2}{G_1 + G_2}$$

where: s_1 = initial entropy of the driving fluid
 s_2 = initial entropy of the driven fluid

In the process, the driving liquid and the driven vapor are accelerated by expanding through nozzles from the respective initial pressures to the mixing pressure. Lines "AB" and "CD" represent the respective reversible expansion processes for the HTW and suction vapor. The two high velocity streams then mix in the converging mixing section. If the two streams are expanded isentropically to the same velocity before mixing, the resulting entropy will be at s_5 and the kinetic energy of the mixture will be equal to (Δh reversible). Isentropic compression along s_5 will increase the pressure to P_5 , at the constant enthalpy line h°_m .

In the case with no friction losses, but where the velocities of the two streams at mixing are different and momentum exchange occurs, there is a loss in available energy and the entropy of the mixture will increase, by an amount equal to Δs_m , to s_4 . The mixture at the mixing pressure and at s_4 would have a kinetic energy equal to (Δh frictionless). Isentropic compression along s_4 would increase the pressure to P_4 . In this process, frictionless but with momentum exchange, the available energy of the two streams has been degraded by an amount:

$$(4) \quad \Delta h_m = (\Delta h \text{ reversible}) - (\Delta h \text{ frictionless}) = T_m (\Delta s_m)$$

where: T_m = absolute temperature at mixing pressure.

For the frictionless process, the value, Δh_m , may be computed from the following equation.

$$(5) \quad \Delta h_m = T_m \Delta s_m = \frac{G_1 G_2 (W_1 - W_2)^2}{(G_1 + G_2)^2} \frac{1}{K^2}$$

where: G_1 = mass flow of HTW
 G_2 = " " " Suction Vapor
 W_1 = velocity of HTW at nozzle exit
 W_2 = velocity of suction vapor at nozzle exit
 K = constant depending on units used

The velocity may be expressed in terms of the isentropic enthalpy changes, Δh_1 and Δh_2 , in the respective expansion nozzles.

$$(6) \quad W_1 = K (\Delta h_1)^{\frac{1}{2}}$$

$$(7) \quad W_2 = K (\Delta h_2)^{\frac{1}{2}}$$

In terms of enthalpy changes the equation for Δh_m becomes:

$$(8) \quad \Delta h_m = T_m \Delta s_m = \frac{G_1 G_2}{(G_1 + G_2)^2} (\sqrt{\Delta h_1} - \sqrt{\Delta h_2})^2$$

The energy degradation, Δh_m , would diminish toward zero as the velocity of the two streams approach equality. This could be done by lowering the mixing pressure or by using a larger quantity of water at a lower initial enthalpy. However, both actions increase friction losses so that a balance is required to obtain maximum performance.

In the actual process with friction, the two entering streams expand by a polytropic path to the mixing pressure with unequal velocities. In this case the entropy of the mixture is further increased by Δs_{f1} , to a value between s_4 and s_3 . Polytropic compression to the actual discharge pressure, P_3 , occurs with an additional entropy increase, Δs_{f2} . Thus friction and turbulence in the two nozzles, mixing chamber and diffuser result in an additional degradation of the available energy as shown by Δs_f , ($\Delta s_f = \Delta s_{f1} + \Delta s_{f2}$).

For the real process, the total loss of available energy results from irreversible mixing and friction. This may be estimated by modifying equation (8) to include the efficiencies of the driving nozzle, suction nozzle, and diffuser, η_1 , η_2 and η_3 respectively. (η_1 , η_2 and η_3 are defined later in this section.)

$$(9) \Delta h_m + \Delta h_f = (\Delta h \text{ reversible}) - (\Delta h \text{ actual}) =$$

$$= \frac{G_1 \Delta h_1 + G_2 \Delta h_2}{G_1 + G_2} - \eta_3 \left[\frac{G_1 (\eta_1 \Delta h_1)^{\frac{1}{2}} + G_2 (\eta_2 \Delta h_2)^{\frac{1}{2}}}{G_1 + G_2} \right]^2$$

The above equation assumes that complete mixing and momentum exchange takes place in expanding to the mixing pressure.

From the above, it is seen that a degradation of input available energy or an increase in entropy occurs from two sources; first, Δs_m or Δh_m is a theoretical loss resulting from the process path, that is irreversible mixing with unequal velocities; second, Δs_f resulting from friction and turbulence in the nozzles, mixing chamber and diffuser.

From the above processes, several efficiencies or reversibility coefficients should be considered. These are defined below. The h-s diagram in Figure 20 also shows calculated values of the various changes in available energy based on the data of test 104. The test data (see Figures 14 and 17) are fairly typical of the high performance tests. Based on these data, calculations are shown below for each efficiency that is defined.

Process Reversibility - expresses the reversibility limitation resulting from the process path, that is irreversibly mixing two streams travelling at unequal velocities.

$$R_1 = \frac{\Delta h \text{ frictionless}}{\Delta h \text{ reversible}} = \frac{31.86}{37.49} = 85\%$$

For the suction, discharge and pressure conditions of test 104, even a process without friction and turbulence losses, the process would be no better than 85% of a reversible process.

Equipment Reversibility - expresses the reversibility limitation resulting from friction and kinetic energy losses, in the nozzles, mixing chamber and diffusor.

$$R_2 = \frac{\Delta h \text{ actual}}{\Delta h \text{ frictionless}} = \frac{19.87}{31.86} = 62.38\%$$

Total Path Reversibility - expresses the reversibility limitation resulting from both irreversible mixing and friction losses:

$$R_3 = R_1 \times R_2 = \frac{\Delta h \text{ actual}}{\Delta h \text{ reversible}} = \frac{19.87}{37.49} = 53.0\%$$

The above efficiencies are concerned with the effectiveness of the process path and with how well the equipment performs in following the process path. An additional efficiency is needed to evaluate the end result since only a part of the work shown by any of the three paths is devoted to compressing the vapor from the suction to the discharge pressure. The useful work actually done by any of the three paths, is only that portion in compressing from the suction to the discharge pressure. This work is shown by the available energy changes, or Δh , above the suction pressure, that is (Δh^* actual) for the actual process, and (Δh^* rev) for the reversible process. From this viewpoint the overall efficiency may be defined as:

$$E^1 = \frac{\Delta h^* \text{ actual}}{\Delta h^* \text{ reversible}} = 1 - \frac{\Delta s \text{ total}}{\Delta s \text{ maximum}}$$

$$E^1 = \frac{11.5}{29.5} = 40.0\%$$

This efficiency expresses the ratio of the actual available energy of the discharge mixture to the reversible available energy, in reference to the suction temperature. In the above " Δs maximum" is the maximum entropy increase that would be possible in the process if no useful compression work were done, that is, if the discharge pressure were equal to the suction pressure.

The overall efficiency in more common use is based on the change in available energy of the two entering streams taken in reference to the discharge temperature and pressure. For the actual process in Figure 20, the value Δh^*_2 represents the increase in available energy of the suction vapor or the minimum compression work done per lb. of suction vapor. Likewise, line Δh^*_1 represents the change in available energy of HTW driving liquid, or the work input per lb. of HTW in expanding down to the discharge pressure. From this the overall efficiency, E, is defined as follows:

$$E = \frac{G_2 \Delta h^*_2}{G_1 \Delta h^*_1} = \frac{\text{Work done on process fluid}}{\text{Work input in driving fluid}}$$

$$E = \frac{(1) (14.53) \text{ BTU}}{(0.756) (61.23) \text{ BTU}} = 31.5\%$$

From the above it may be seen that while the equipment is 63% efficient in following the process path, it is 31.5% efficient in accomplishing the desired work. This results from the fact that the equipment must work over a much longer path (greater changes in available energy) than is theoretically necessary just to do the desired compression. This longer path is unavoidable since the driving fluid must be expanded to some pressure below the suction pressure to achieve mixing.

Three individual component efficiencies should also be considered. These are shown below:

1. The efficiency, η_1 , of the HTW expansion through the driving nozzle from P_1 to the mixing pressure; based on enthalpy change of the HTW in expanding to the mixing pressure, P_m ;

$$\eta_1 = \frac{\text{actual enthalpy change}}{\text{isentropic enthalpy change}}$$

2. The efficiency, η_2 , of the suction nozzle in allowing expansion of the suction vapor to the mixing pressure:

$$\eta_2 = \frac{\text{actual enthalpy change in vapor}}{\text{isentropic enthalpy change in vapor}}$$

3. The efficiency, η_3 , of the diffusor in converting kinetic energy to obtain a pressure increase from P_m .

$$\eta_3 = \frac{\text{actual enthalpy change}}{\text{isentropic enthalpy change}}$$

As expressed earlier, the individual component efficiencies cannot be computed from the existing data because the (1) velocity of the liquid and vapor are not equal, (2) the flow is not all in one direction, and (3) the velocity profiles over the various cross section are not known. We do know from the previous analysis that the combined effect of the component efficiencies is equal to R_2 , (62.38%).

While it is not possible to divide these efficiencies, the rather high computed efficiencies of the diffusor and driving nozzle and other previous work suggest that the greatest losses occur in the mixing process.

VI. SUMMARY

The test data has shown that the actual performance of the test jet was higher than was anticipated. Still, it is expected that further improvements, (15 to 20% increase in the reversibility, R_3), would result from additional tests. This would be possible from improvement in the individual component efficiencies and adjustments in the process path.

FIGURE 2
PRESSURE INSTRUMENTS

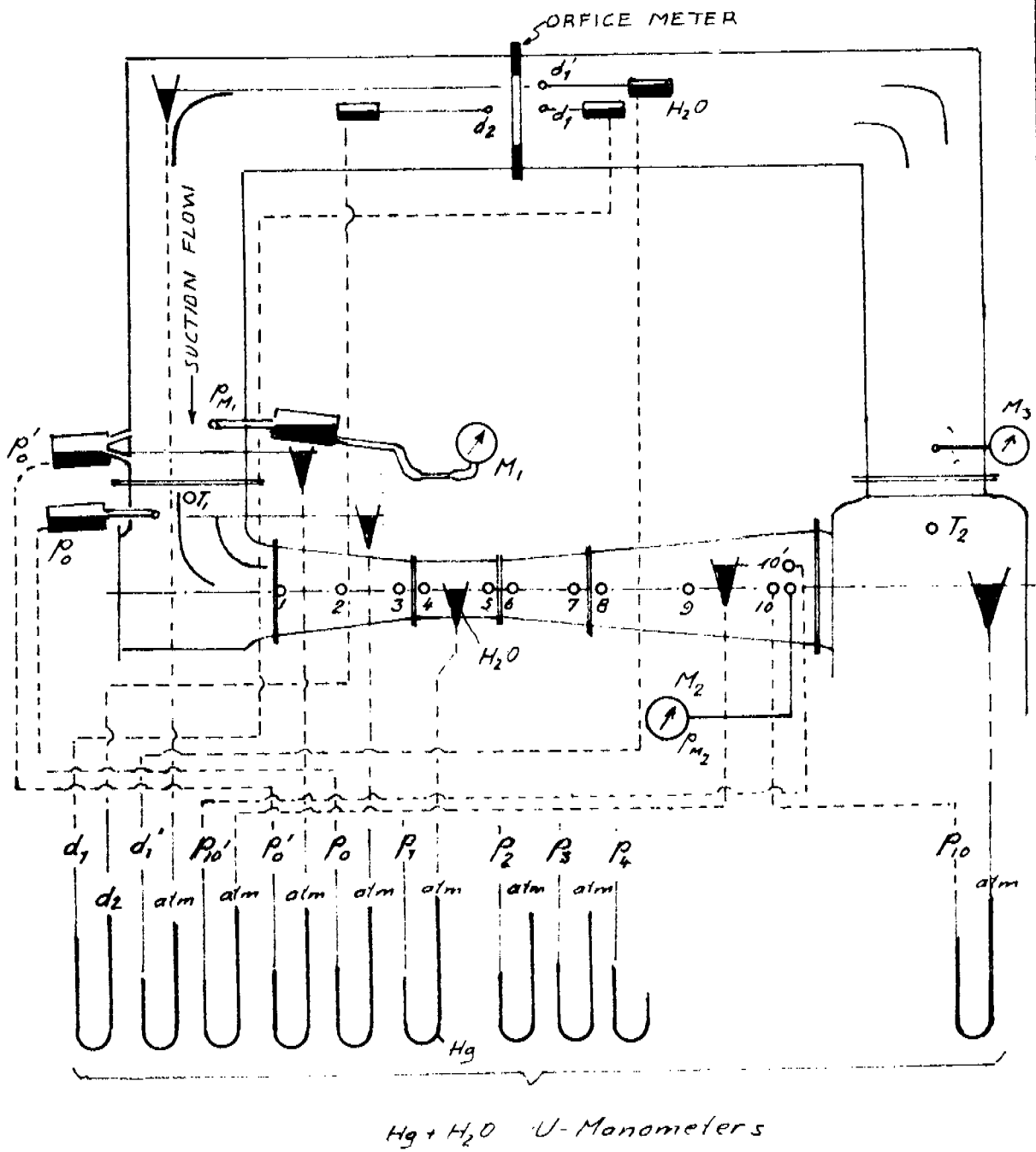
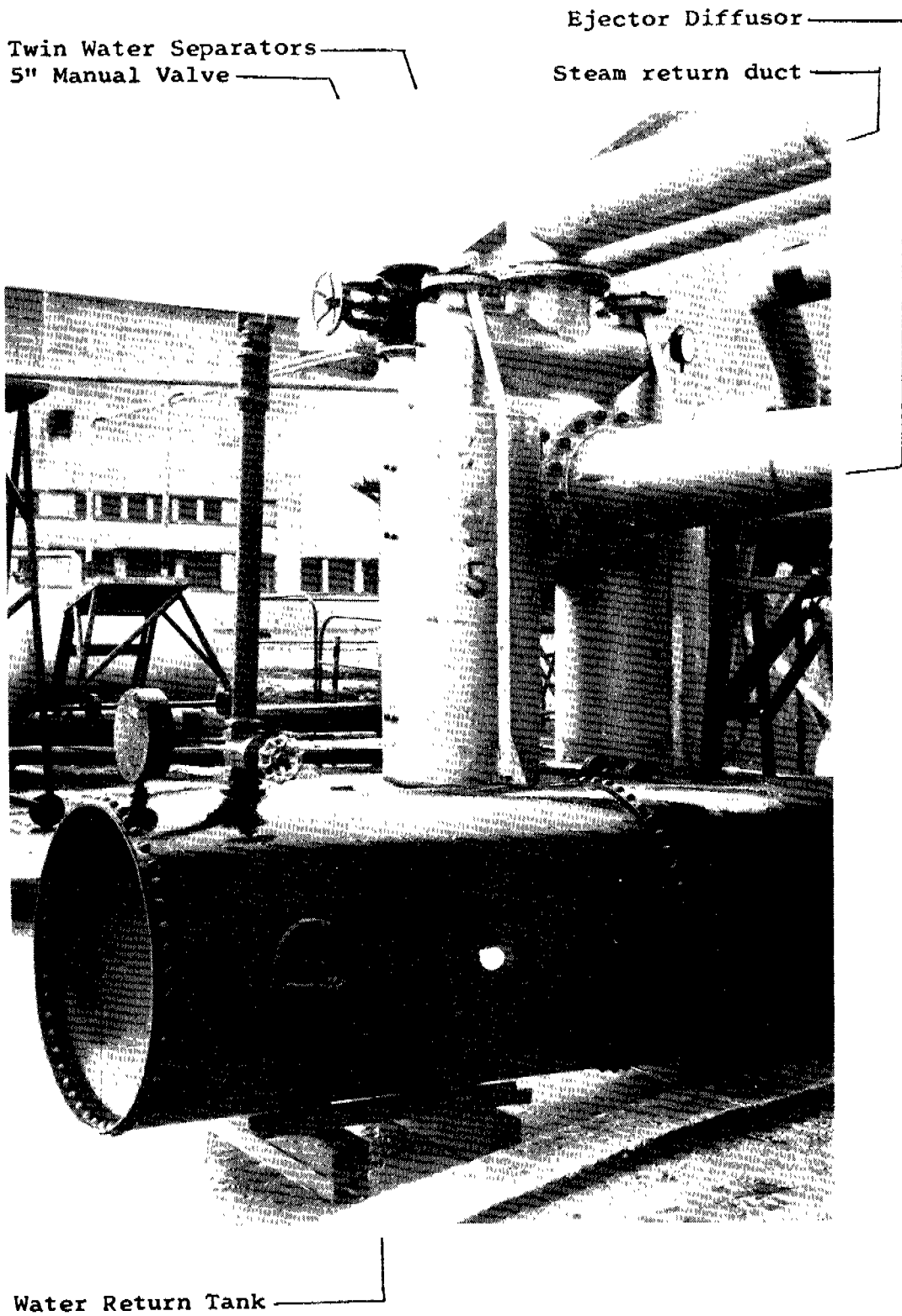


Figure 3

DISCHARGE END OF TEST JET
READY FOR HYDROSTATIC PRESSURE TEST

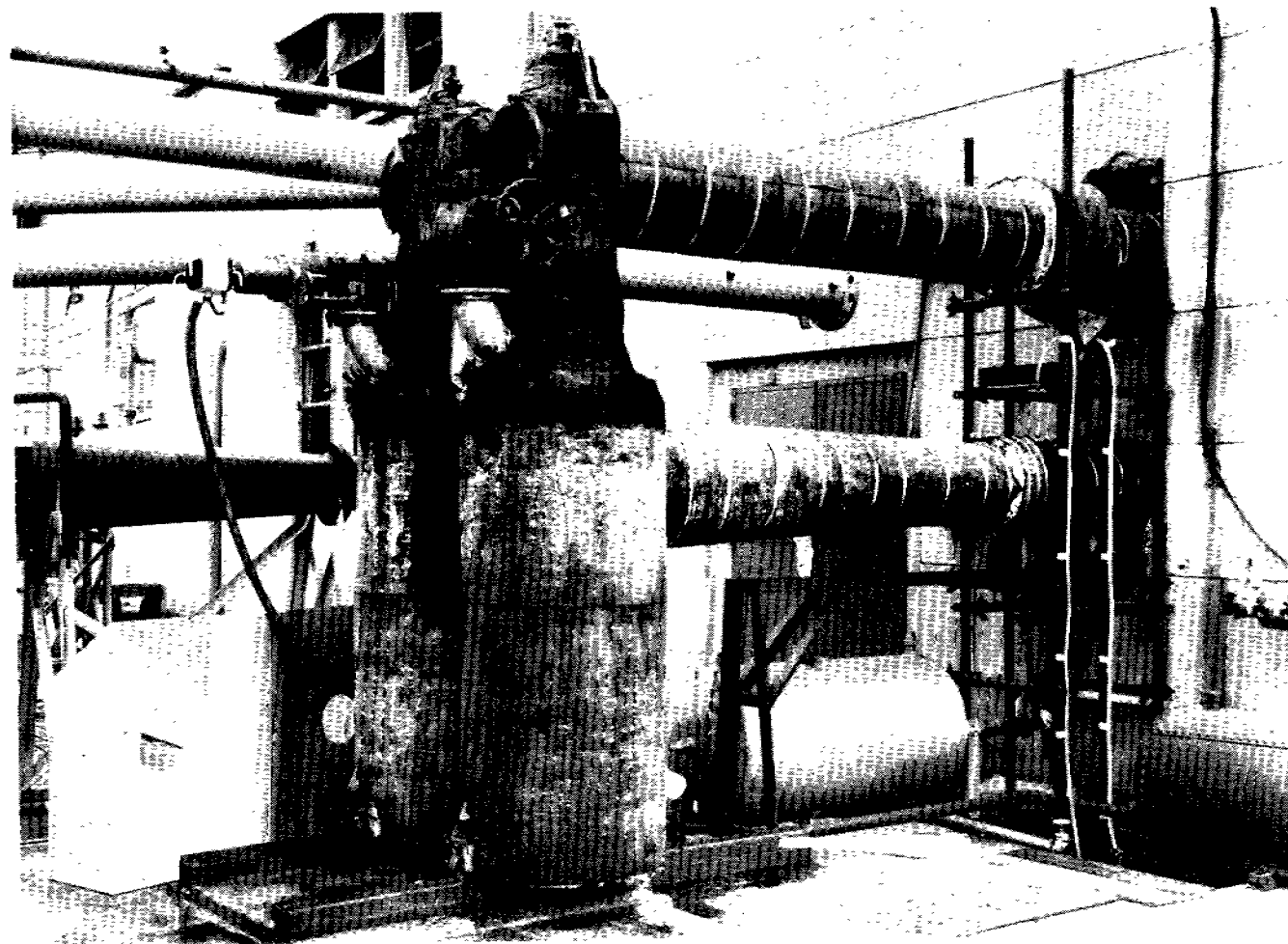


Automatic Discharge
Pressure Control
Valve

Safety Valves

Suction Steam
Flow Orifice

Deflectors
For Safety
Valves
Removed



Separators on Rails

Water Return
Duct

DISCHARGE END OF TEST JET READY FOR TEST

FIGURE 4

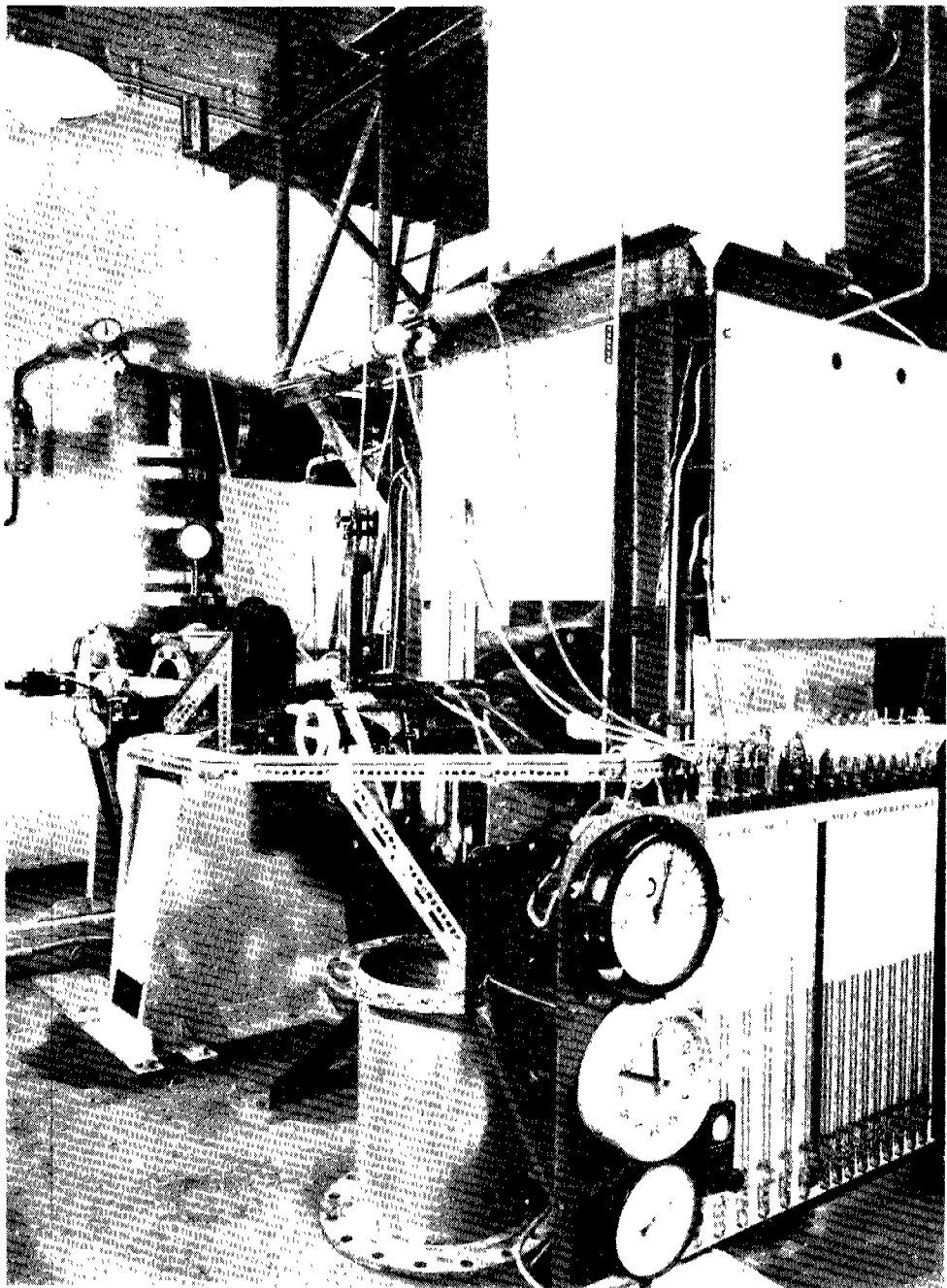
Figure 4

INSTRUMENTATION AND GENERAL
ARRANGEMENT OF TEST JET

Suction Steam
Duct

Hot Water Accumulator

Warm Up
Steam
Line



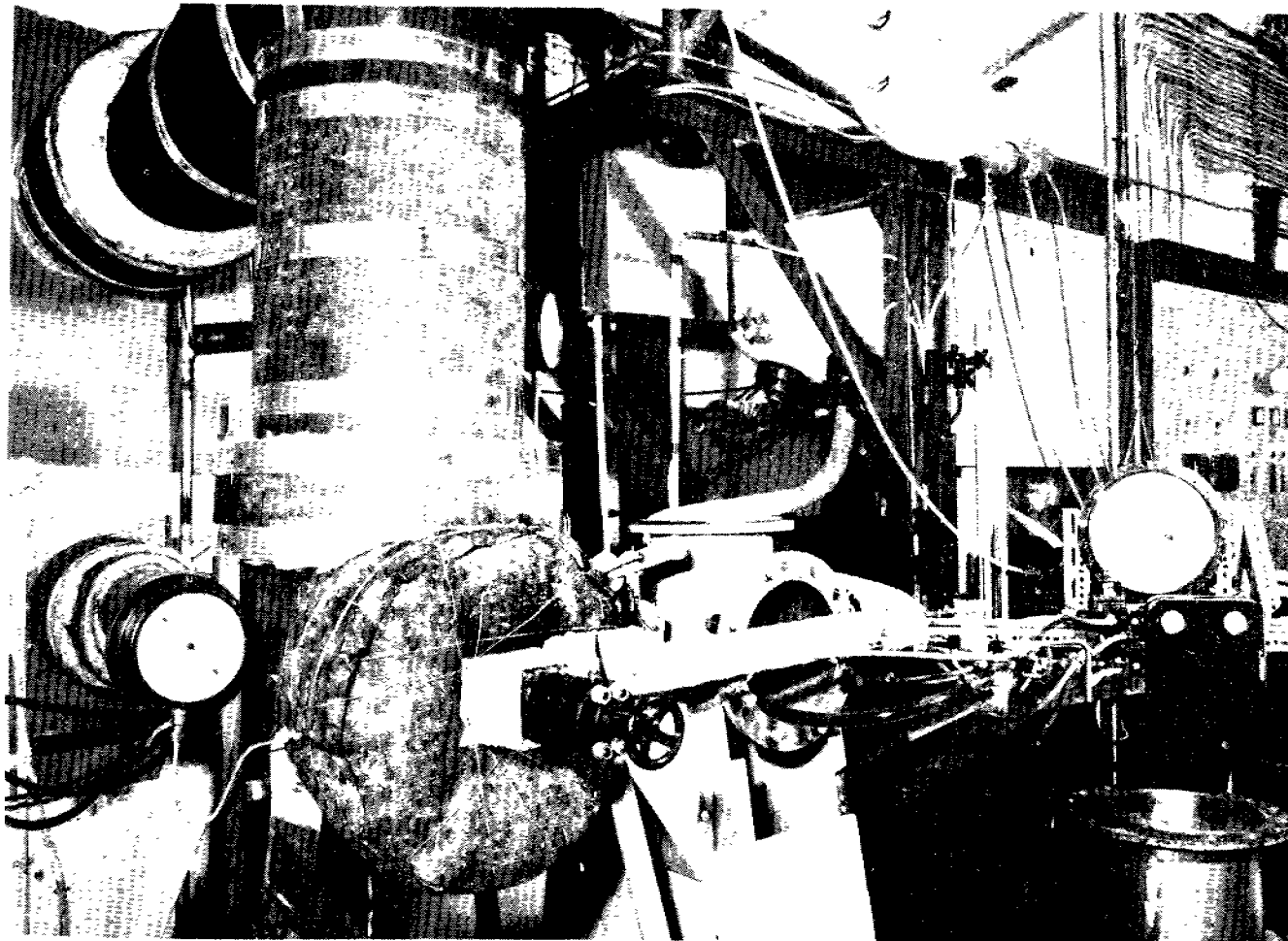
Hydraulically Operated
Hot Water Needle Valve
At Driving Nozzle

Instrument Panel for
Photographic Recording
-HTW Accumulator Level
-Time - HTW Pressure
-Manometers

Butterfly Valve For
Suction Pressure
Control

HTW Accumulator

7/20



Suction Piping &
Nozzle Chamber

HTW Nozzle &
Needle Valve

HTW Pipe to
Nozzle (White)

SUCTION END OF JET READY FOR TEST

FIGURE 6

Figure 6

MATERIAL & ENERGY BALANCE FOR HTW JET

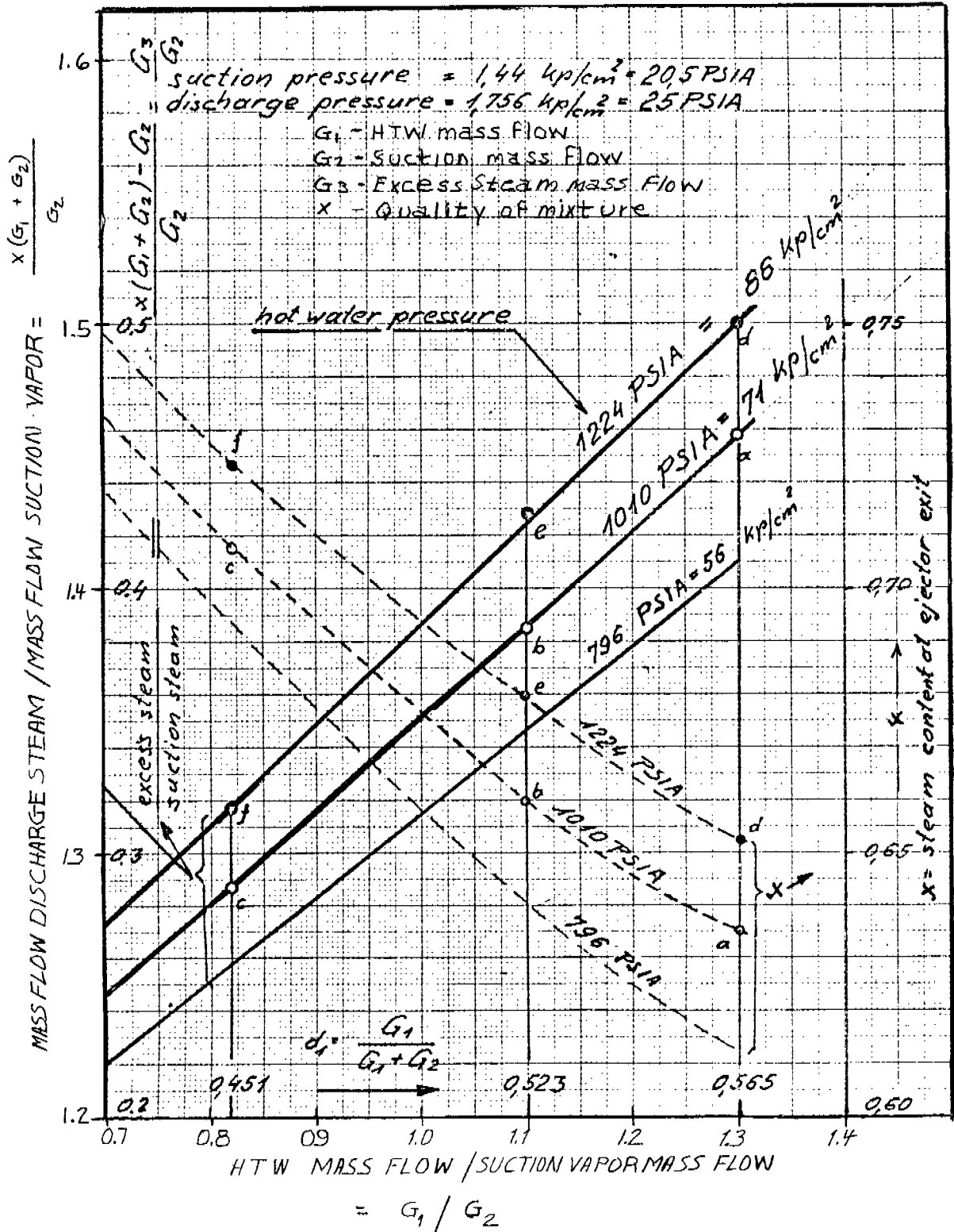
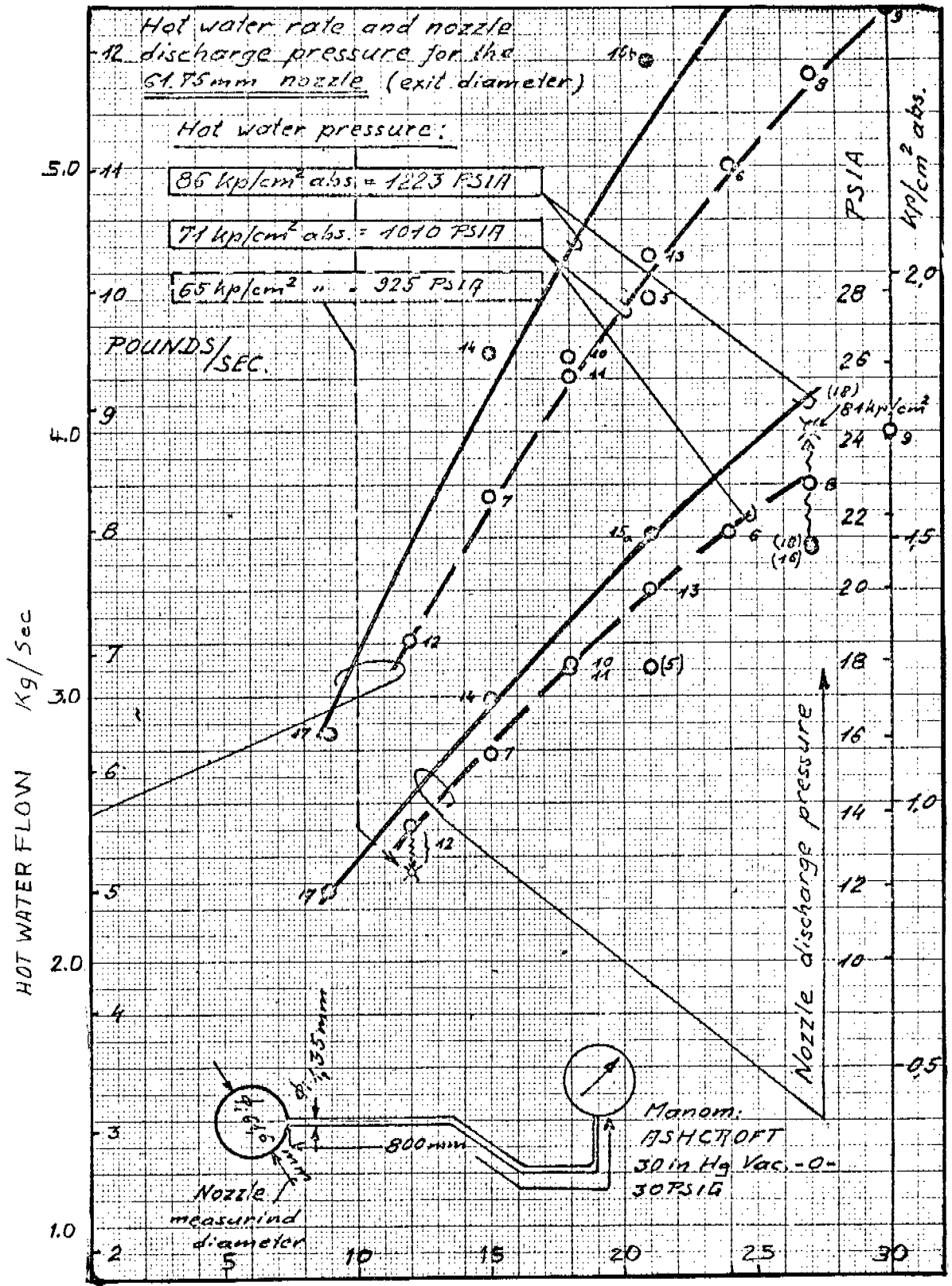


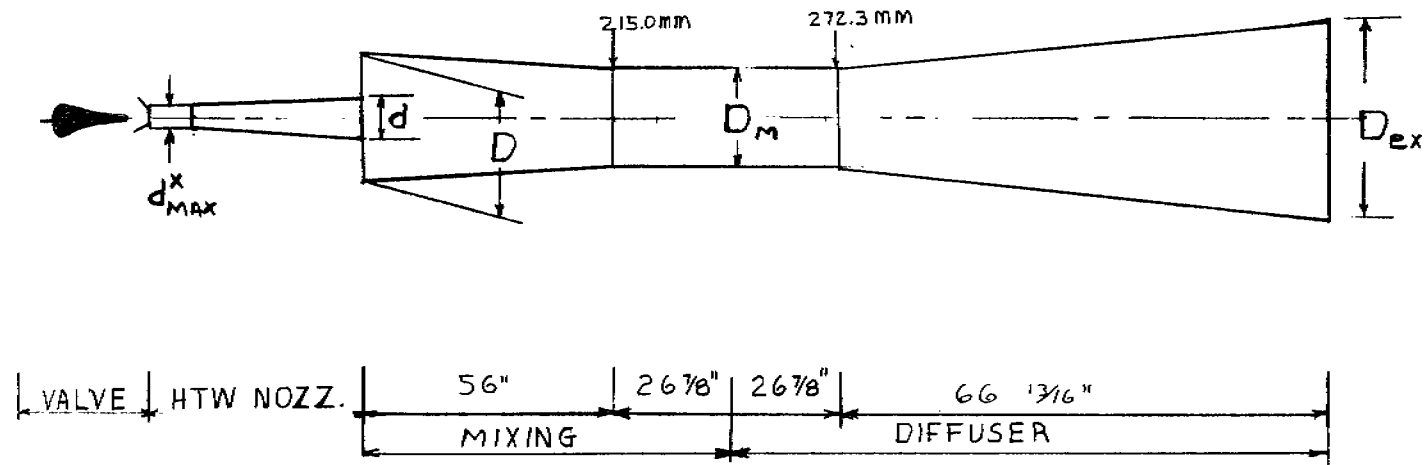
FIGURE 8

HTW DRIVING NOZZLE CALIBRATION



∅ = NEEDLE VALVE OPENING - mm

FIG. 9 TEST EJECTOR



DIMENSIONS -

d^x_{MAX}	D_{ex}	D_M	D	d	
15.5	457.2	217.4	320.5	61.8	mm
0.61	18	8.54	12.6	24.25	INCHES

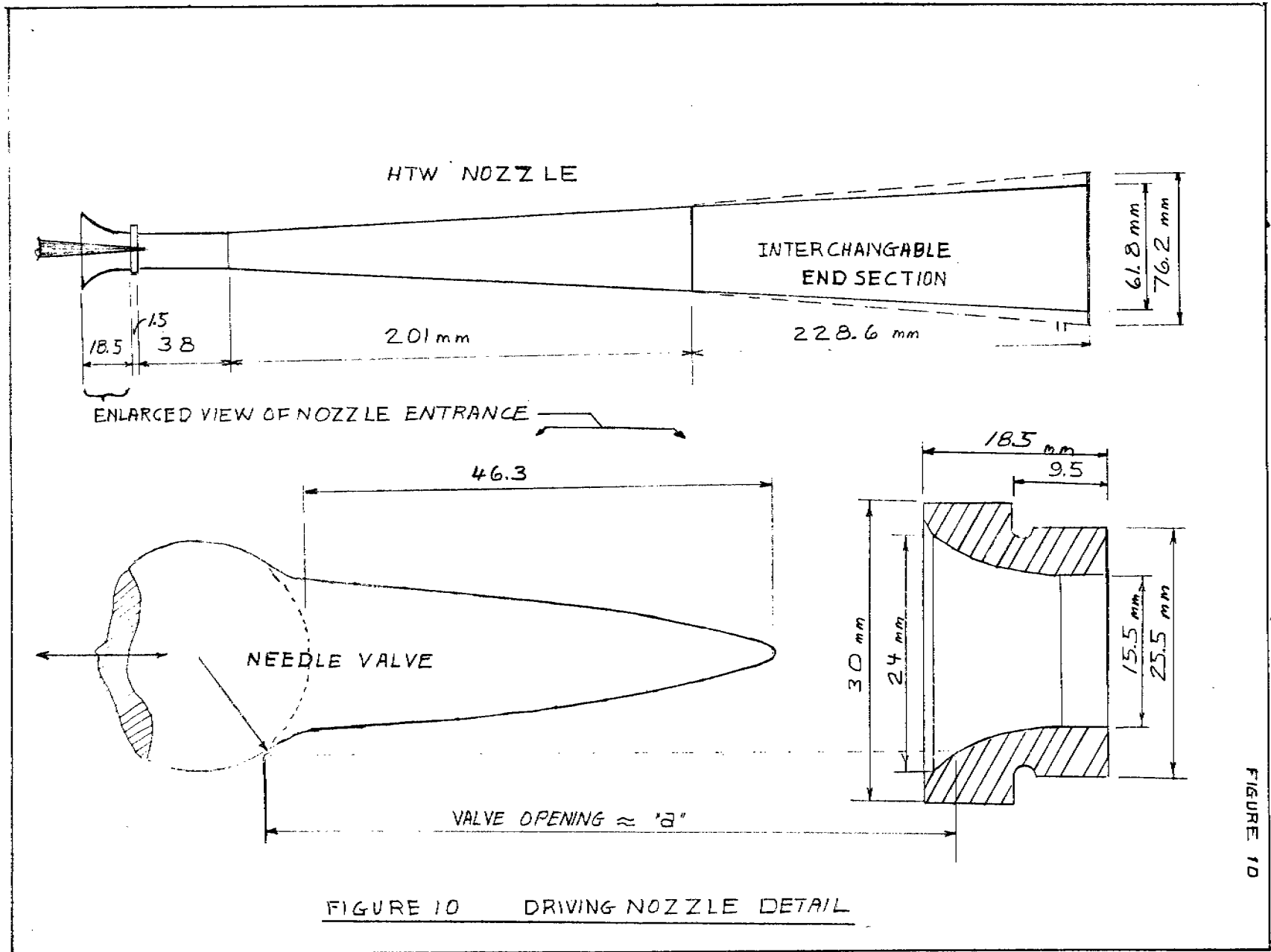


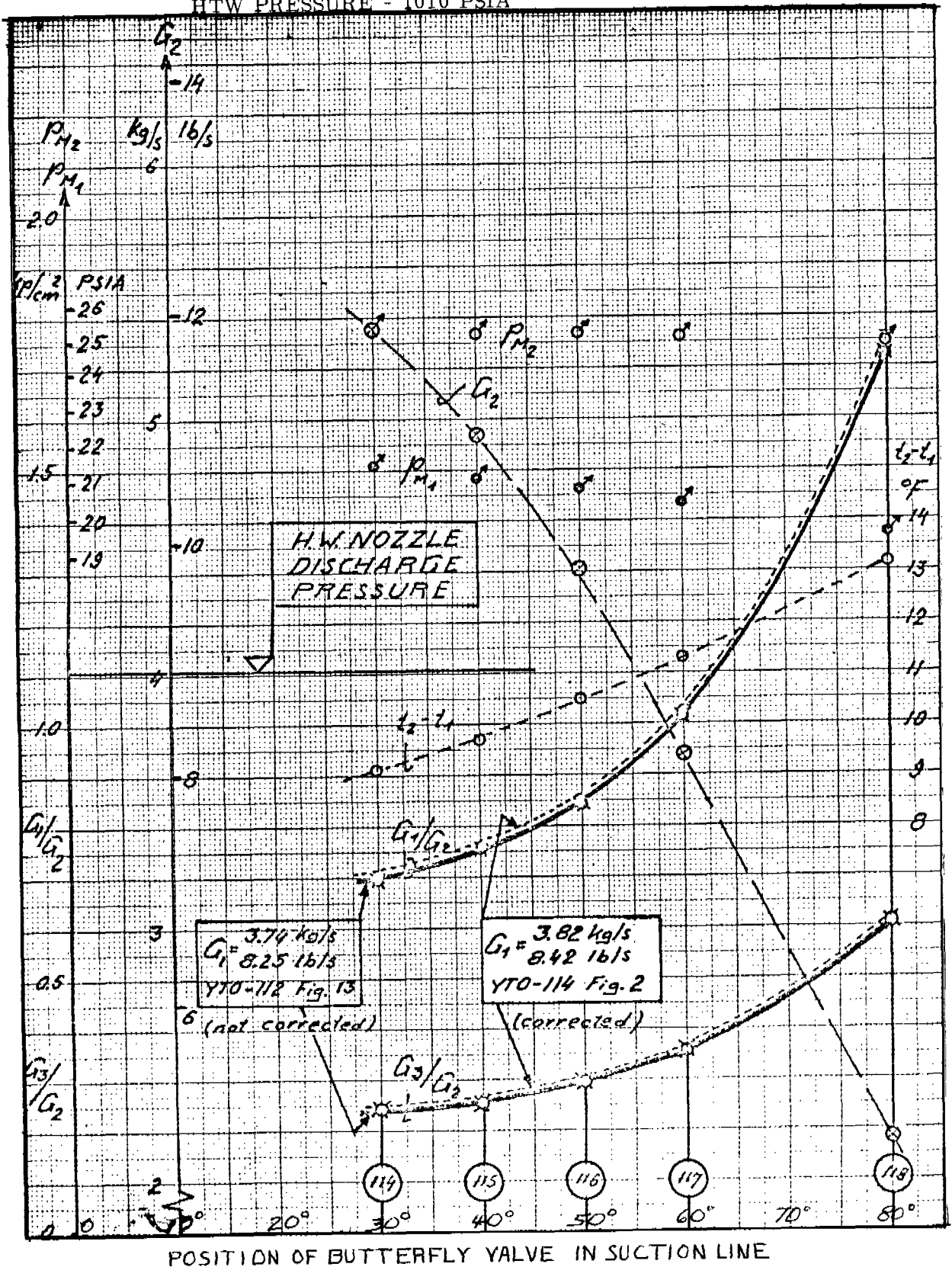
FIGURE 11

COMPARISON OF TEST RESULTS AT BEST PERFORMANCE

Test Nozzle Size - mm	$\frac{G_3}{G_2}$ $t_2 - t_1$	Pressure - psia		$t_2 - t_1$	G_2 lbs. /Sec.	G_1/G_2	G_3/G_2
		Suction	Discharge				
76.2	.0241	12.35	16.06	12.9	9.04	0.85	0.31
61.8	.0238	20.77	25.46	11.1	14.26	0.757	0.265
Estimated Performance	.0278	20.5	25	10.8		0.863	0.30

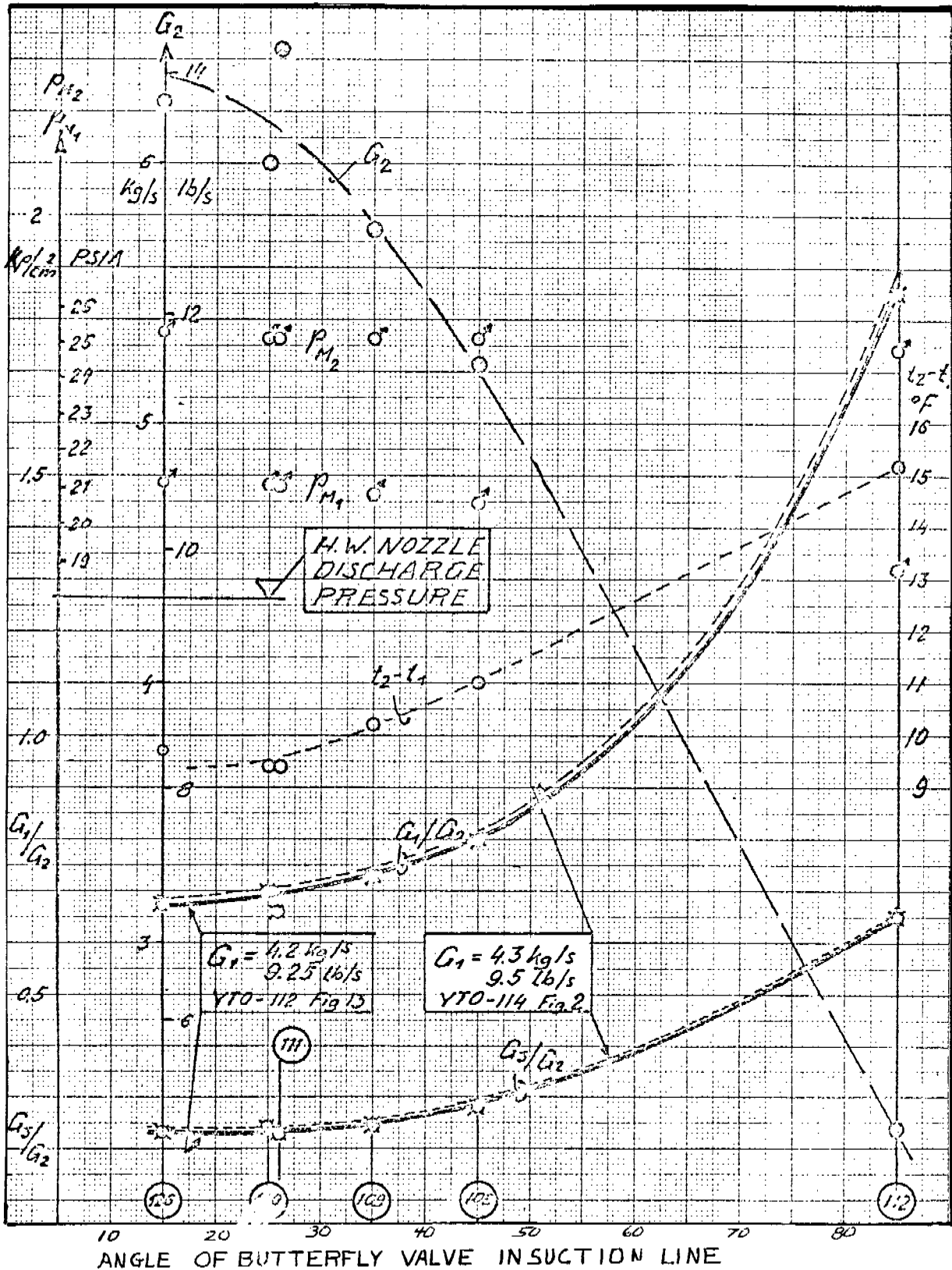
TEST DATA - 61.8 MM NOZZLE
 HTW FLOW = 8.42 lb/sec
 HTW PRESSURE - 1010 PSIA

Figure 12



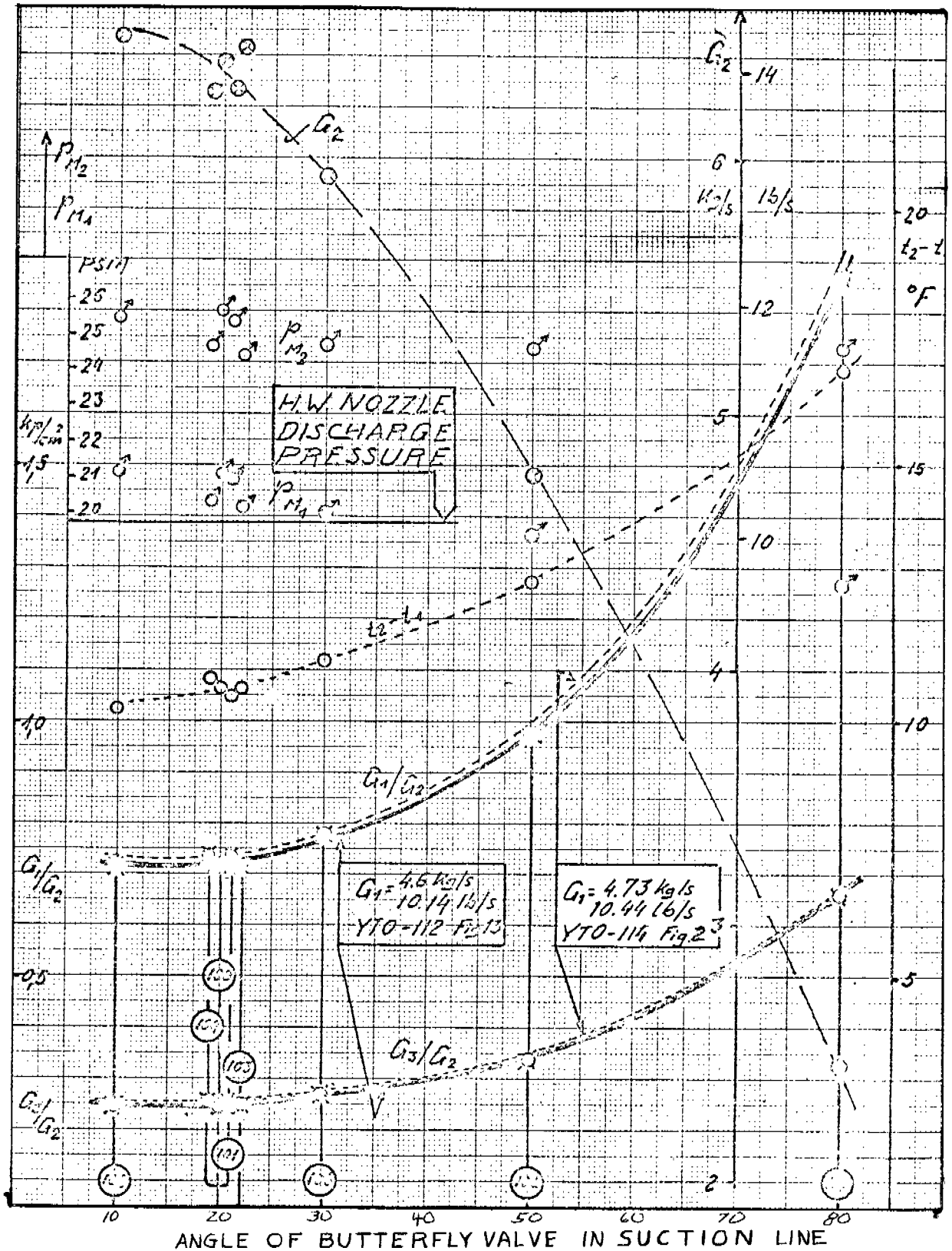
TEST DATA - 61.8 MM NOZZLE
 HTW FLOW = 9.5 lb/sec
 HTW PRESSURE = 1010 PSIA

Figure 13



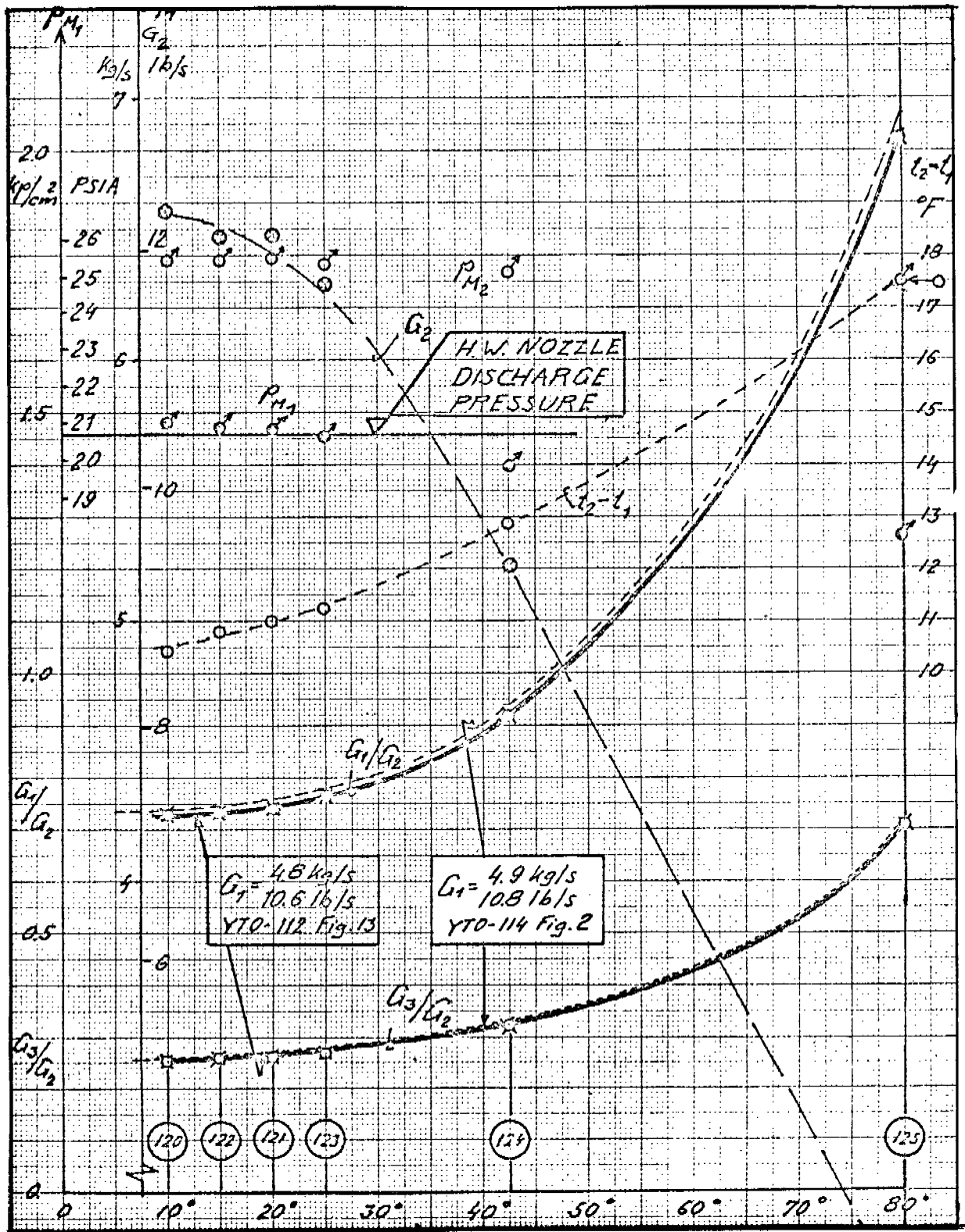
TEST DATA - 61.8 MM NOZZLE
 HTW FLOW = 10.44 lb/sec
 HTW PRESSURE = 101Q PSIA

Figure 14



TEST DATA - 61.8 mm Nozzle
 HTW FLOW = 10.8 lb/sec
 HTW PRESSURE = 1010 PSIA

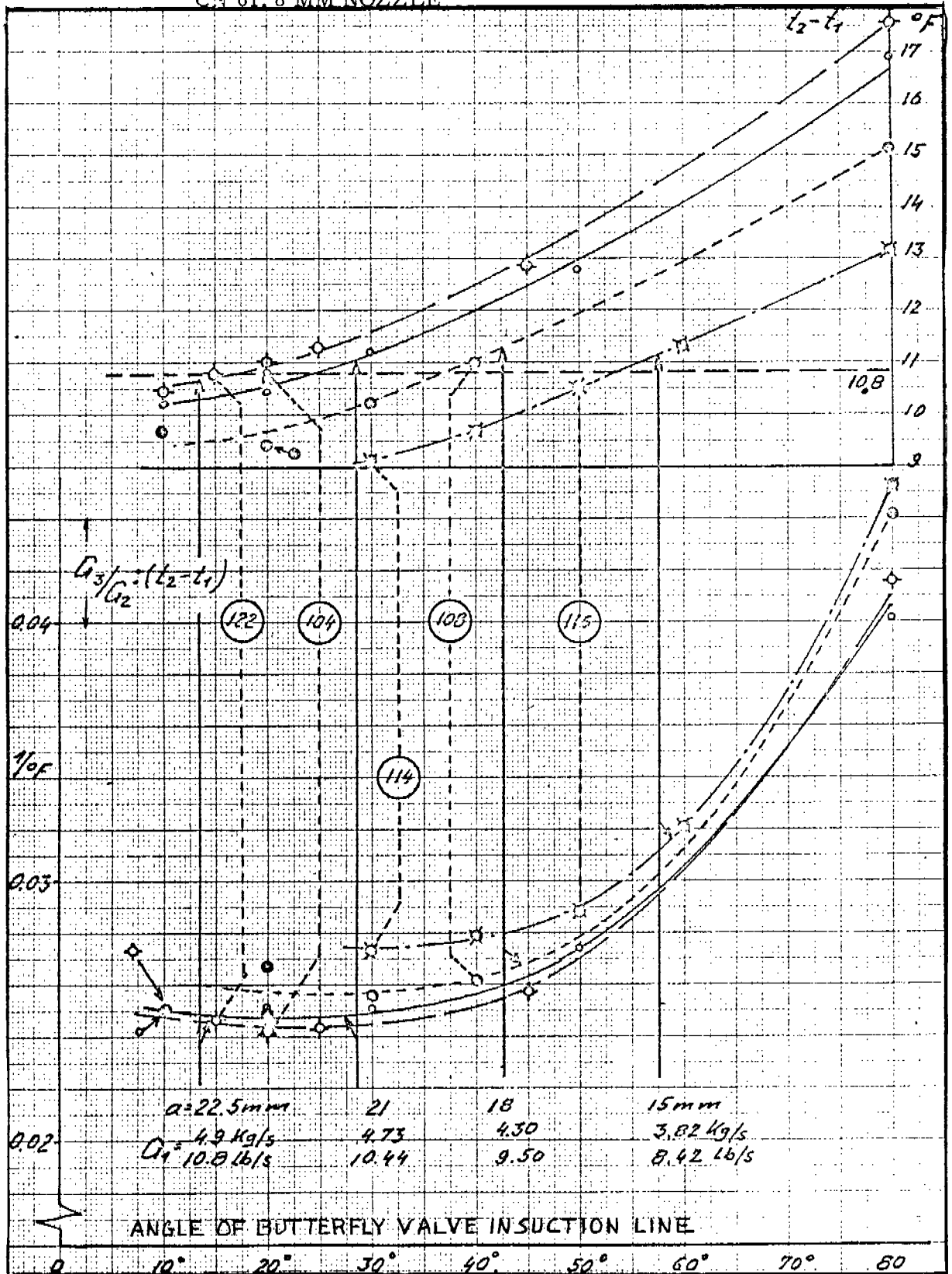
Figure 15



Angle of Butterfly Valve in Suction Line

PERFORMANCE RATIOS FOR TEST
CN 61. 8 MM NOZZLE

Figure 16



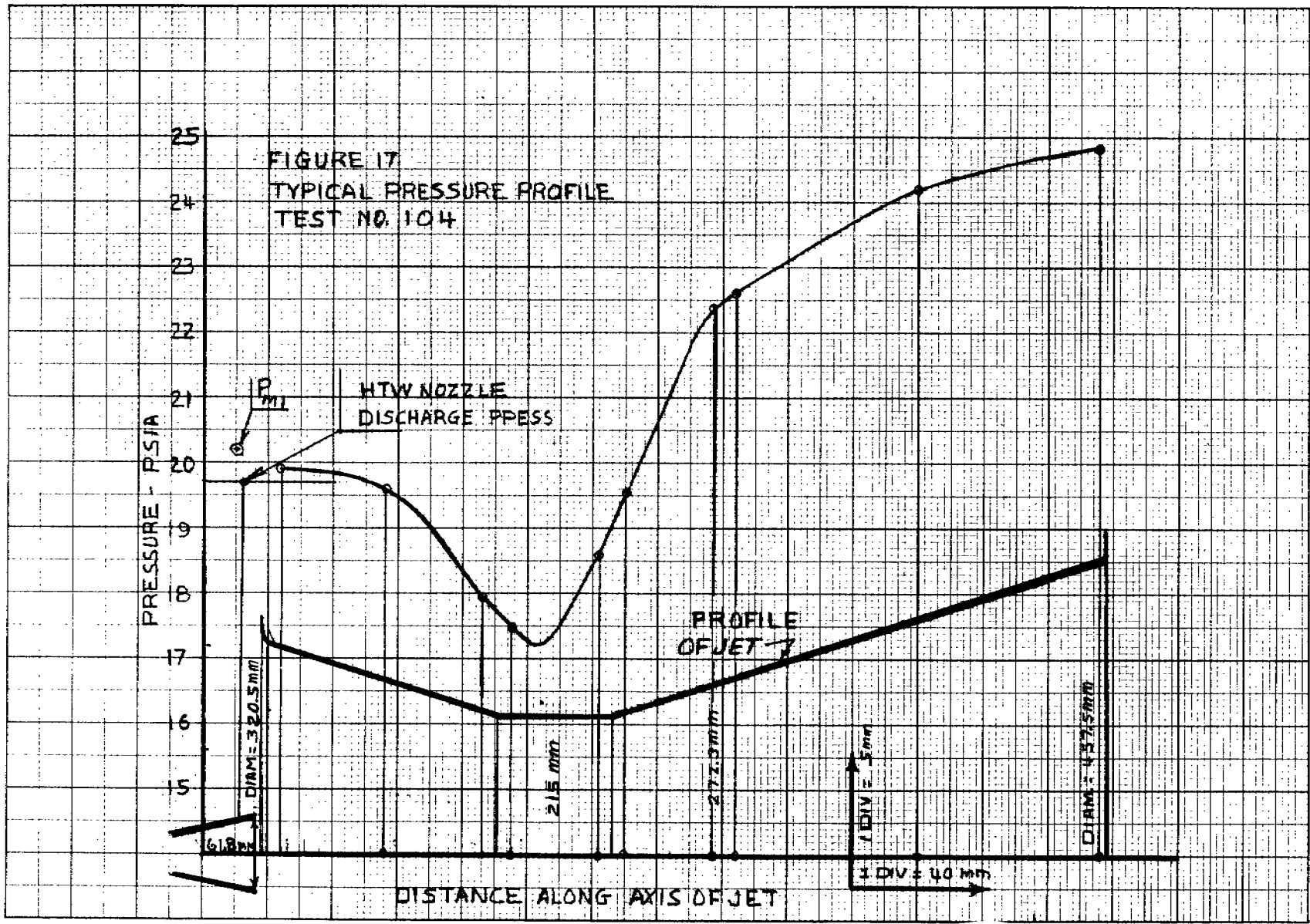
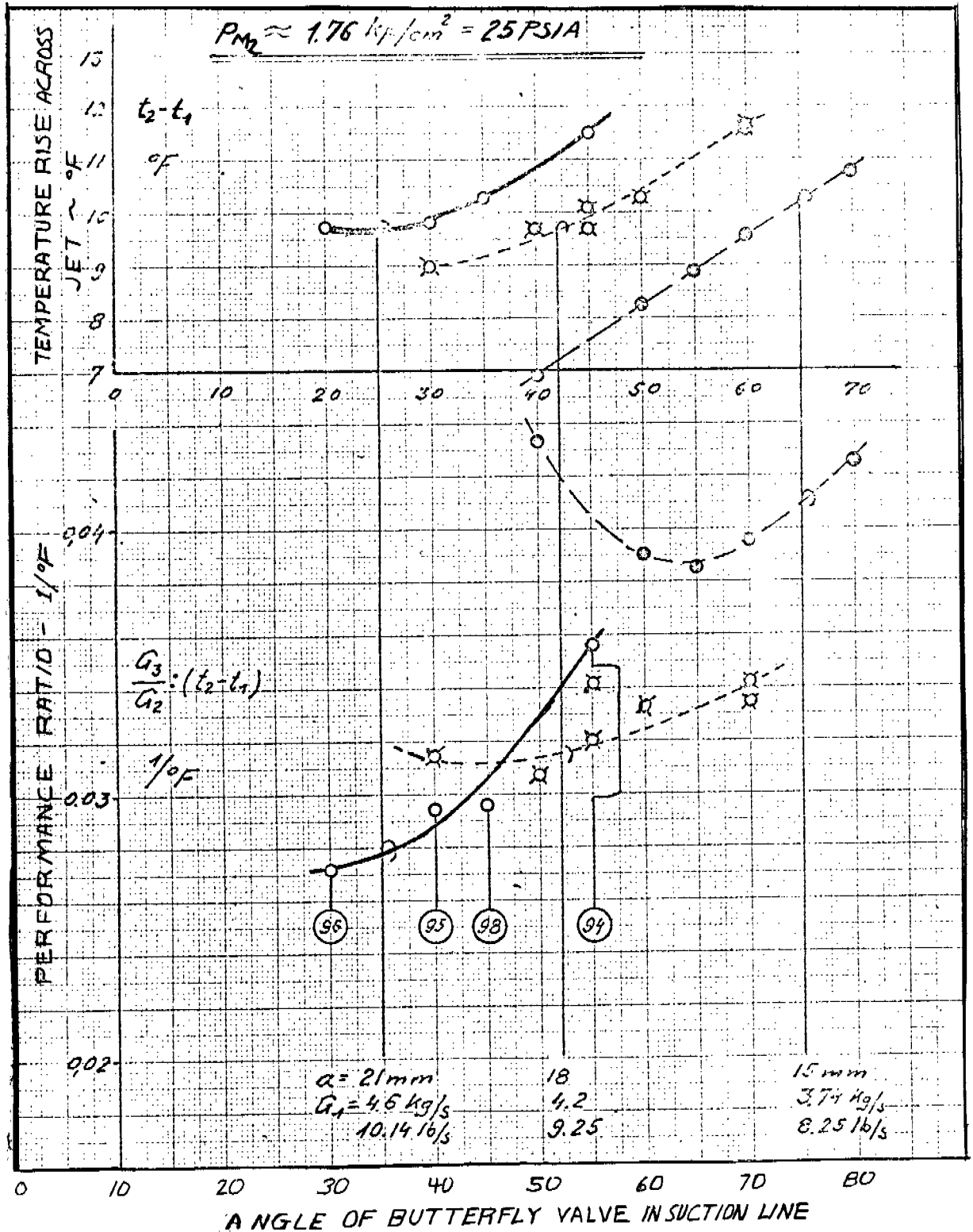


FIGURE 17

PERFORMANCE RATIOS FOR TEST ON 76.2 MM NOZZLE
 HTW PRESSURE = 1010 PSIA
 DISCHARGE PRESSURE = 25 PSIA

Figure 18



PERFORMANCE RATIOS FOR TEST ON 76.2 MM NOZZLE
 HTW PRESSURE = 1010 PSIA
 DISCHARGE PRESSURE = 16.06 PSIA

Figure 19

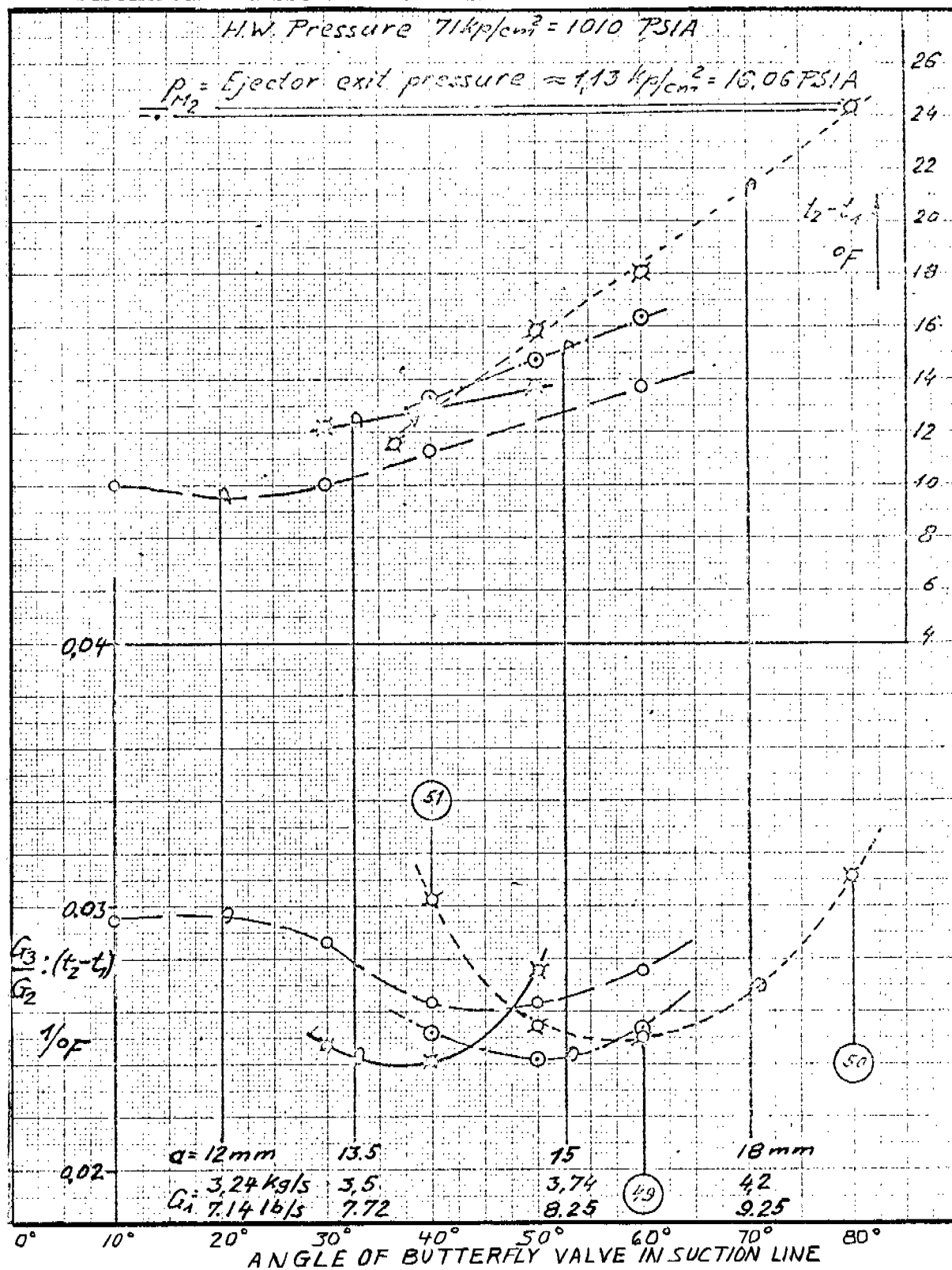


FIGURE 20 ENTHALPY-ENTROPY DIAGRAM

DATA FROM TEST 104

SUCTION PRESS 20.28 PSIA

DISCHARGE PRESS 24.80

MIXING PRESS 17.30

$G_1 : G_2 = 0.756$ LBS HTW PER LB SUCTION VAPOR

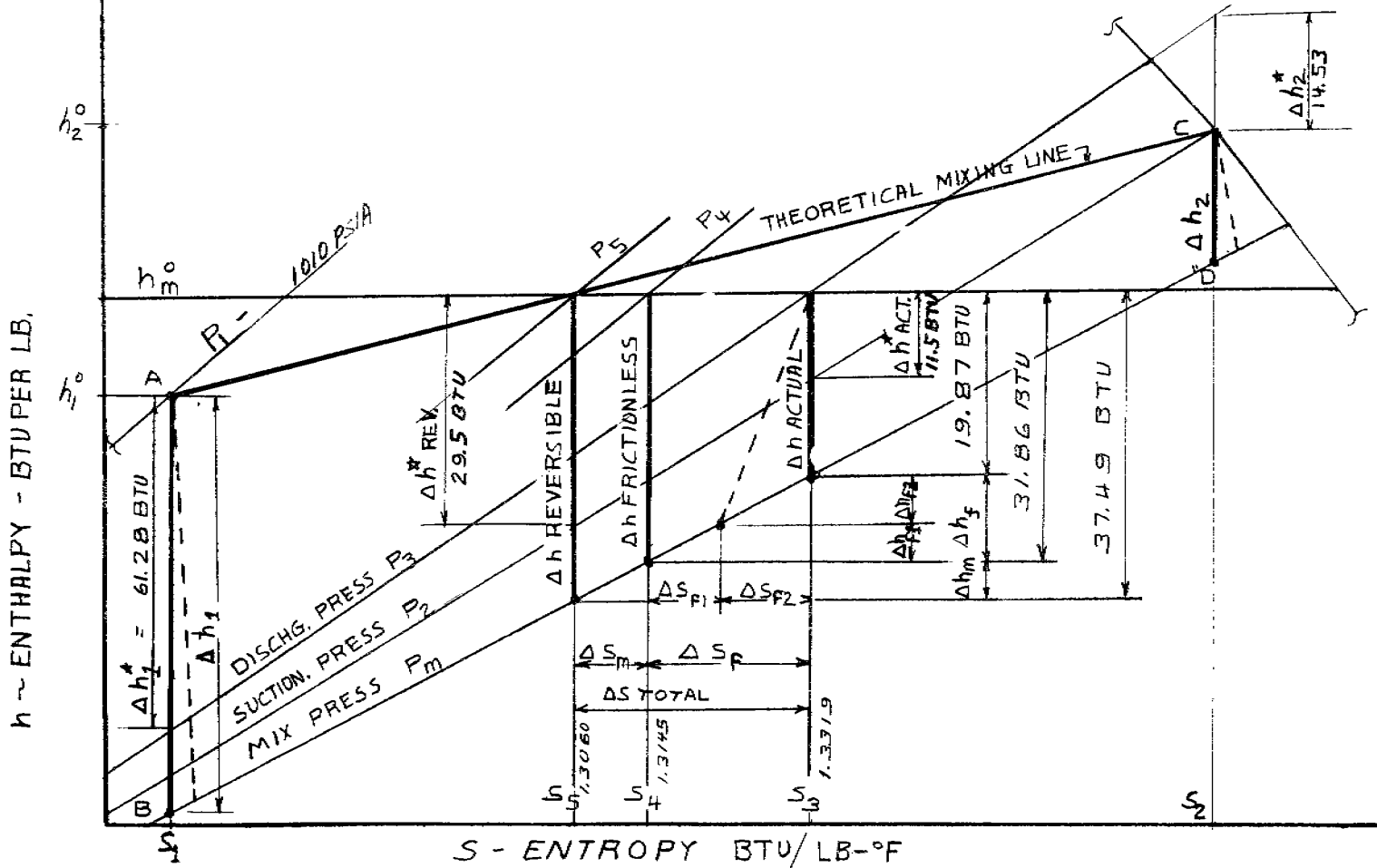


FIGURE 20